DOI: 10.1111/1750-3841.17182

#### ORIGINAL ARTICLE

Food Science WILEY

Check for updates

Food Chemistry

### Using transglutaminase to cross-link complexes of lactoferrin and $\alpha$ -lactalbumin to increase thermal stability

Yufeng Zhou<sup>1</sup> | Tiantian Lin<sup>1</sup> | Younas Dadmohammadi<sup>1</sup> | Peilong Li<sup>1</sup> | | Lixin Yang<sup>1</sup> | Yanhong He<sup>1</sup> | Gopinathan Meletharayil<sup>2</sup> | Hongmin Dong<sup>1</sup> Rohit Kapoor<sup>2</sup> Alireza Abbaspourrad<sup>1</sup>

#### Correspondence

Alireza Abbaspourrad, Department of Food Science, College of Agriculture and Life Sciences, Cornell University, Ithaca, NY 14853, USA.

Email: alireza@cornell.edu

#### **Funding information**

Dairy Management Inc; National Science Foundation, Grant/Award Number: DMR-1719875

#### **Abstract**

The poor thermal stability of lactoferrin (LF) hinders its bioavailability and use in commercial food products. To preserve LF from thermal denaturation, complexation with other biopolymers has been studied. Here we present the complex formation conditions, structural stability, and functional protection of LF by  $\alpha$ lactalbumin ( $\alpha$ -LA). The formation of the LF- $\alpha$ -LA complexes was dependent on pH, mass ratio, and ionic strength. Changing the formation conditions and cross-linking by transglutaminase impacted the turbidity, particle size, and zetapotential of the resulting complexes. Electrophoresis, Fourier-transform infrared spectroscopy, and circular dichroism measurements suggest that the secondary structure of LF in the LF- $\alpha$ -LA complex was maintained after complexation and subsequent thermal treatments. At pH 7, the LF- $\alpha$ -LA complex protected LF from thermal aggregation and denaturation, and the LF retained its functional and structural properties, including antibacterial capacity of LF after thermal treatments. The improved thermal stability and functional properties of LF in the LF- $\alpha$ -LA complex are of interest to the food industry.

#### KEYWORDS

lactoferrin, protein-protein complexation, thermal stability, transglutaminase,  $\alpha$ -lactalbumin

#### INTRODUCTION 1

Globular proteins offer the food industry a wide variety of food functionality, but their uses are currently limited because of their structural instability to thermal processing, ultrasonication, and homogenization (Yang et al., 2021). These proteins form soluble or insoluble aggregates

Yufeng Zhou and Tiantian Lin equally contributed toward this manuscript.

and gel upon thermal denaturation, pH fluctuation, and ionic strength changes at high protein concentrations, all of which present issues for their use in the food, cosmetic, and pharmaceutical industries (Nicolai, 2016; Yang et al., 2014). Given these problems, various delivery systems and methods have been developed to encapsulate and protect globular proteins for controlled release and to maintain ideal rheological, optical, or sensorial properties (Yang et al., 2021).

This is an open access article under the terms of the Creative Commons Attribution-NonCommercial License, which permits use, distribution and reproduction in any medium, provided the original work is properly cited and is not used for commercial purposes.

© 2024 The Author(s). Journal of Food Science published by Wiley Periodicals LLC on behalf of Institute of Food Technologists.

<sup>&</sup>lt;sup>1</sup>Department of Food Science, College of Agriculture and Life Sciences, Cornell University, Ithaca, New York, USA

<sup>&</sup>lt;sup>2</sup>Dairy Management Inc., Rosemont, Illinois, USA

Lactoferrin (LF) is an 80 kDa single-chain glycoprotein with 689 amino acid residues (Lin et al., 2021). It is an ironrich globular protein that has shown significant biological activity including acting as an iron delivery agent and possessing antibacterial properties (Taheri-Kafrani et al., 2009). It has been proposed that LF's high affinity for iron competes with bacteria impeding bacterial growth, and the cationic patches on LF's surface interact with Lipid A stimulating the production of lipopolysaccharide, which damages bacterial cell walls (Jenssen & Hancock, 2009). While interest in using LF as a natural bioactive ingredient has increased, LF has proven to be unstable at high temperatures losing both its ability to deliver iron as well as its antibacterial properties (Harouna et al., 2020). Unfortunately, LF is denatured at most food processing temperatures, apo-LF (<15% of iron) denatures at  $\sim70^{\circ}$ C, natural-LF (15%-20% of iron) between 70 and 90°C, and holo-LF (>20% of iron) at ~90°C. Denaturing causes LF to lose both iron content and concomitant with conformational changes, the cationic patches become less available and LF loses its antibacterial properties. Therefore, protecting LF and its nascent properties from various processing conditions, including extreme thermal conditions and the pH fluctuation (Nedovic et al., 2011), is of great interest.

Therefore, we are interested in complexing LF with other proteins and molecules to enhance its thermal stability and improve its applications. One route to improving the stability of LF is to take advantage of its high isoelectric point (pI 8.5-9.2) (Bengoechea et al., 2011). This has made it possible to associate with negatively charged micro and macromolecules (McCarthy et al., 2014). Whey protein isolate (WPI), which has a much lower pI ~5.3, has been shown to have a strong binding affinity with LF, and as a natural byproduct of the dairy industry, finding new uses for whey would contribute to a more sustainable food chain (Darmawan et al., 2020). WPI contains three main ingredients:  $\beta$ -lactoglobulin,  $\alpha$ -lactalbumin ( $\alpha$ -LA), and bovine serum albumin (Barbana et al., 2006).  $\alpha$ -LA is a 14.2 KDa whey protein with a single chain of 123 amino acid residues (Huppertz et al., 2004) and has high affinity toward hydrophobic peptides (Kehoe & Brodkorb, 2014). The unique structure of  $\alpha$ -LA with 4 disulfide bonds and no thiol groups provides thermal stability to the protein (Lin et al., 2021). The pI of  $\alpha$ -LA is 5.3, which means that it would be negatively charged at pH levels between pH 5.3 to 8.5 where LF would be positively charged and therefore could form electrostatic complexes (Barbana et al., 2006).

To enhance and strengthen these electrostatic interactions and improve the yield of LF– $\alpha$ -LA complexes, we will also investigate the use of transglutaminase (TG), a nontoxic transferase that catalyzes  $\varepsilon$ -( $\lambda$ -glutamyl)-lysyl bonds intra and intermolecular between lysine and glutamine residues in proteins (Salinas-Valdés et al., 2015). Studies have shown that TG cross-links  $\alpha$ -LA to form larger  $\alpha$ -

LA particles (Matsumura et al., 2000), and TG can also cross-link LF to improve LF's ability to stabilize Pickering emulsions (Xia, 2022).

We hypothesized that by forming a complex between LF and  $\alpha$ -LA through electrostatic interactions and then cross-linking the proteins using TG, the bacterial and functional properties of LF would be protected at temperatures and conditions used during food processing. Here, we report our investigation of the complex formation conditions between LF and  $\alpha$ -LA and their cross-linking with TG; we evaluate the complex formation efficiency and yield, then evaluate the thermal stability, structural conformation, and antibacterial properties of these complexes in comparison to native LF.

#### 2 | MATERIALS AND METHODS

#### 2.1 | Materials

The bovine LF powder (Iron >15 mg/100 g; natural bovine LF, Bioferrin 2000, purity  $\sim$  96.7%) was donated by Glanbia Nationals, Inc, and the  $\alpha$ -LA (purity >91.0%) was donated by AGROPUR. Sodium hydroxide (purity >97.0%) and hydrochloric acid (12 M) were purchased from Fisher Scientific. TG was purchased from Modernist Pantry. A vertical mini gel electrophoresis system and 2X Laemmli buffer were purchased from Bio-Rad. Sodium dodecyl sulfate (SDS) (purity >98.5%) was purchased from Sigma-Aldrich. The Luria broth (LB) was purchased from Sigma-Aldrich.

### 2.2 | Preparation of LF- $\alpha$ -LA complex

#### 2.2.1 | Stock solution preparation

Stock solutions of LF and  $\alpha$ -LA at 1.0 w/v % were prepared by dissolving LF and  $\alpha$ -LA in Milli-Q water and stirring at 800 rpm at room temperature (25°C) for 1 h. To ensure complete hydration, both prepared solutions were stored overnight at 4°C. Then, samples of each protein stock solution were adjusted to target pH levels (5.8, 6.0, 6.5, and 7.0) using 0.1 M HCl or 0.1 M NaOH.

### 2.2.2 | LF- $\alpha$ -LA complex preparation

Mixtures with different ratios of LF to  $\alpha$ -LA at target pH levels were made (8:1, 6:1, 4:1, 2:1, 1:1, 1:2, 1:4, 1:6, and 1:8 (LF:  $\alpha$ -LA)). Then, after an additional incubation period of 30 min at 25°C, the turbidity, zeta-potential, and particle size were measured. Different methods were used to find optimal ratios at different pH levels to enhance the yield of the complexes by incubating the LF- $\alpha$ -LA mixtures at



0.5, 4, or 8 h at  $45^{\circ}$ C. The mixtures after incubation were collected by centrifugation at  $4^{\circ}$ C at 15,000 g for 30 min and then frozen ( $-20^{\circ}$ C) and freeze-dried (Labcono). Freeze-dried samples were then redispersed in PBS buffer prior to thermal studies.

### 2.2.3 | TG-LF-a-LA complex preparation

The LF- $\alpha$ -LA mixtures with the highest turbidity formed at pH 6.0 and 6.5 were incubated at room temperature (25°C) for 0.5 h, followed by adding a different amount of TG with extra 8-h incubation at 45°C. The cross-linked with TG (TG-LF- $\alpha$ -LA) complexes were initially collected as the same condition (centrifugation at 4°C at 15,000 g for 30 min and then frozen (-20°C) and freeze-dried).

### 2.2.4 | Control solutions for thermal treatments

Stock solutions of LF,  $\alpha$ -LA, and direct mix (DM) samples were used as controls for thermal treatments. DM samples were prepared by dissolving LF and  $\alpha$ -LA in PBS (pH 7.0, 10 mM) and mixing by 2:1, 1:1, and 1:2 (LF: $\alpha$ -LA) and used without centrifugation, freeze-drying, and pH adjustment.

# 2.3 | Thermal treatment LF- $\alpha$ -LA complexes

LF– $\alpha$ -LA complexes (pH 6.5 formed 2:1, pH 6.0 formed 1:1 and 1:2) were rehydrated using 0.2 w/v % in PBS (pH 7, 10 mM). TG cross-linked samples, TG–LF– $\alpha$ -LA complexes (10 mg TG cross-linked pH 6.5 formed 2:1, pH 6.0 formed 1:1 and 1:2) were also prepared for thermal treatments in 0.2 w/v % in PBS buffer (pH 7, 10 mM). Controls were 0.2 w/v %, 0.15 w/v %, and 0.1 w/v % LF, and 0.2 w/v %  $\alpha$ -LA solutions in PBS (pH 7, 10 mM). Each solution (2 mL) was loaded into glass test tubes, and then thermal treatments were conducted (75 or 90°C) in a water bath for 2 min;100 s to reach equilibrium temperature, then held at temperature for 20 s. The samples were immediately cooled in an ice-water bath until they reached 25°C.

# 2.4 | Physicochemical characterization of complexes

### 2.4.1 | Turbidity

Turbidity was measured using the method published by Lin et al. (2022). Briefly, the transmittance was measured at 600 nm in 1 cm path-length quartz cuvettes by a UV–Vis light spectrophotometer (UV-2600, SHIMADZU Co.) at

25°C. The blank was Milli-Q water (100% transmittance). The calculation of solution turbidity was calculated using the following equation:

$$T = -\ln \frac{I}{I_0} \tag{1}$$

where I is the sample transmittance intensity, and  $I_0$  is the blank transmittance intensity.

#### 2.4.2 | Particle size

The particle diameter and size distribution of LF,  $\alpha$ -LA, and LF- $\alpha$ -LA and TG-LF- $\alpha$ -LA complexes were done using the procedures according to Lin et al. (2022) without modification.

### 2.4.3 | Zeta-potential

The zeta-potentials of the LF,  $\alpha$ -LA and LF- $\alpha$ -LA, and TG-LF- $\alpha$ -LA solutions were measured by Nano-ZS in Smoluchowski mode. All measurements were carried out in triplicate.

#### 2.4.4 | Intrinsic fluorescence spectra

Intrinsic fluorescence was measured using a Shimadzu RF-6000 spectrophotometer (Shimadzu) using a 1-cm quartz cuvette. All heated and unheated LF- $\alpha$ -LA and TG-LF- $\alpha$ -LA complexes (0.2 w/v %,) and LF (0.2 w/v %, 0.15 w/v %, and 0.1 w/v %) were prepared in the PBS buffer (pH 7.0, 10 mM). The excitation wavelength was 295 nm, and the emission was measured over the range of 310–400 nm. The slit widths for excitation and emission were both 10 nm.

# 2.4.5 | Fourier-transform infrared spectroscopy (FTIR) analysis

Fourier-transform infrared spectroscopy (FTIR) was carried out on an IRAffinity-1S Spectrometer with a single reflection attenuated total reflectance accessory from the Shimadzu Corporation. An average of 32 scans from 400 to 4000 cm<sup>-1</sup> with a resolution of 4 cm<sup>-1</sup> were collected.

# 2.5 | Far-UV circular dichroism (CD) spectroscopy analysis

The change of LF secondary structure after complexation and thermal treatments was analyzed by circular



dichroism (CD) spectroscopy. AVIV-202-01 spectropolarimeter (Lakewood, NJ, USA) in the far-UV region (190–260 nm) was applied to measure all 0.2~W/v% samples in a quartz cell with a 1-mm path length at  $25^{\circ}\text{C}$ .

### 2.6 | Electrophoresis analysis

The electrophoresis analysis followed the method from Lin et al. (2022) with some modifications. At first, the mixture of the same volume of samples (2 mg mL $^{-1}$  of protein) and 2× Laemmli buffer was incubated at 50°C for 4 h in a water bath. Second, the electrophoresis process was processed in 150 V for 120–150 min.

### 2.7 | Optical microscopy

An aliquot ( $\sim$ 0.3 mL) of each of LF,  $\alpha$ -LA, and LF- $\alpha$ -LA complexes and TG-LF- $\alpha$ -LA was transferred to a glass microscope slip and covered with a glass coverslip. The optical microscopy images were observed by light microscope (Leica DM IL LED) equipped with a camera (Vision Research, AMETEK, Miro Lab 3a10) under a 20× magnification lens (Leica HI Plan). The images were analyzed by ImageJ software (version 1.52a).

# 2.8 | Scanning electron microscopy (SEM)

Fresh suspensions of LF, DM mixtures, or LF- $\alpha$ -LA complexes and TG-LF- $\alpha$ -LA complexes were either vacuum-dried overnight or freeze-dried before scanning electron microscopy (SEM) analysis (Zeiss Gemini 500). Au/Pd (Denton Desk V) was applied to sputter-coated samples before scanning and photographing by a high-efficiency secondary electron detector under the conditions reported by Lin et al. (2022).

### 2.9 | Antibacterial analysis

The antibacterial activity of the LF– $\alpha$ -LA complexes and TG–LF– $\alpha$ -LA complexes against *Staphylococcus aureus* (*S. aureus*), which was isolated by the Animal Health Diagnostic Center of Cornell University (AHDC) from bovine feces, and *Escherichia coli* K 12 (*E. coli*) was performed on a 96-well microtiter plate (Harouna et al., 2020). The incubated bacteria broth was diluted in Luria-Bertani (LB) broth 1000 times to maintain the absorbance of 100  $\mu$ L bacteria broth less than 0.04 at 625 nm. To each well was added 100  $\mu$ L of diluted bacteria, and 100  $\mu$ L of unheated or heated

LF– $\alpha$ -LA, and TG–LF– $\alpha$ -LA complex solutions. Then, the microtiter plate was incubated at 37°C, and the absorbance was measured at 625 nm to monitor the growth of bacteria after 0, 12, and 24 h of incubation with shaking for 10 s before reading. A 100  $\mu$ L bacteria sample mixed with 100  $\mu$ L PBS buffer was the control, and all sample analysis was performed in triplicate.

### 2.10 | Statistical analysis

The obtained data were presented as means with standard deviation. JMP Pro16 (SAS Institute, USA) was conducted for the analysis of variance and Tukey HSD comparison test (p < 0.05). GraphPad Prism9 was used for figure plotting (GraphPad Software Inc.).

#### 3 | RESULTS AND DISCUSSION

### 3.1 | Formation of LF- $\alpha$ -LA complexes

To form the complexes between LF and  $\alpha$ -LA, we exploited the differences in overall charge between the two proteins. We used zeta-potential analysis of our  $\alpha$ -LA at pH levels between 3.5 and 10 to confirm its pI. We found that the pI of our  $\alpha$ -LA was 5.6, which is a little higher than expected but likely due to small levels of impurities in the sample. Our LF solutions have a positive charge between pH 5.8 and 7.0 because the pI of LF is close to 8.0 (Lin et al., 2022). Therefore, the optimal pH range in which to form LF- $\alpha$ -LA electrostatic complexes was determined to be between 5.8 to 7.0, where the two proteins were oppositely charged. Complex formation was studied at pH levels 5.8, 6.0, 6.5, and 7.0. At each pH, the biopolymer solutions were mixed at a series of mass ratios from 8:1 to 1:8 (LF: $\alpha$ -LA).

The turbidity (A–D) and visual appearance (a–d) of the LF– $\alpha$ -LA complexes were used to choose the best conditions for complex formation (Figure 1). As the pH increased, the turbidity of the samples remained low across all mass ratios. However, lower pH favored higher complex yield as evidenced by the visually observed and measured increase in turbidity. The highest turbidity and observed cloudiness occurred at pH 5.8 and 6.0 at the mass ratios 1:1, 1:2, and 1:4 (LF: $\alpha$ -LA). At higher pH for any mass ratio, the turbidity was low with only slight cloudiness observed at 1:1 at pH 6.5 and for 2:1 at pH 7. We collected the samples with the highest turbidity via centrifugation and then freeze-dried the pellet for future analysis.

To further understand the LF- $\alpha$ -LA complex formation at different mass ratios and pH values, the zeta-potential and the mean particle sizes were measured (Figure 2S A-D and Figure 3S A-D). When the two protein solutions

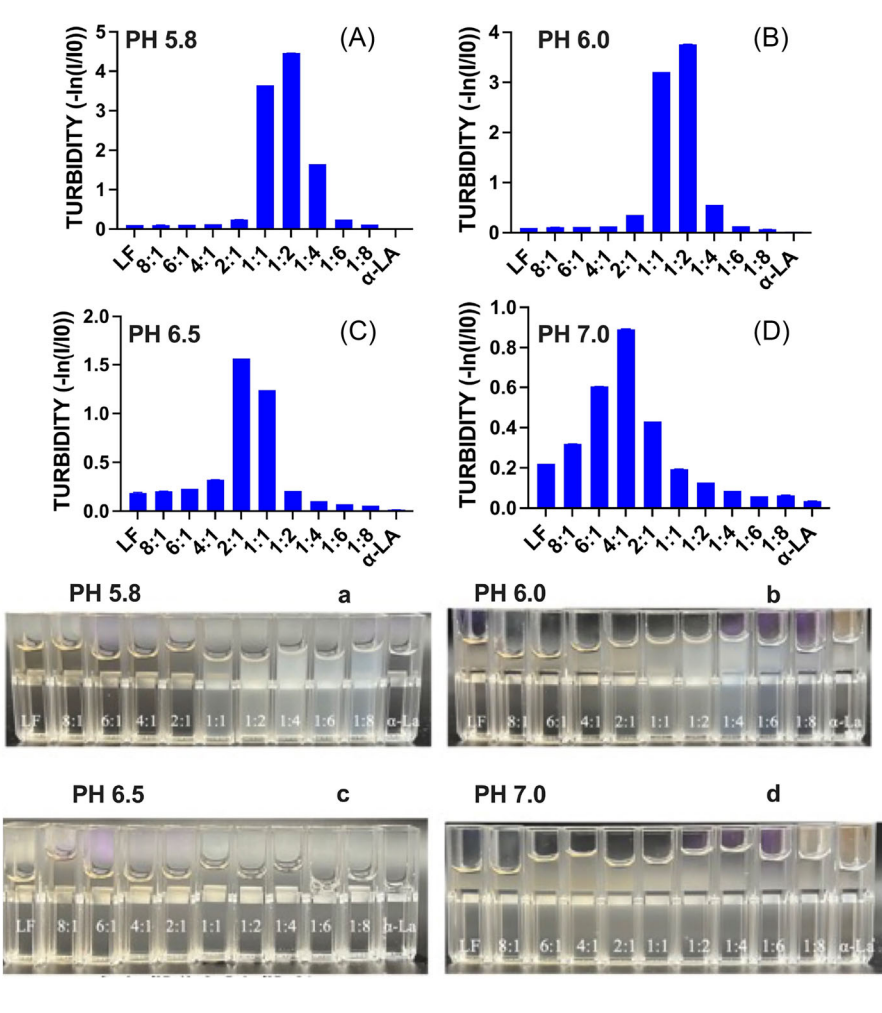


FIGURE 1 Turbidity and optical images of lactoferrin (LF)–α-lactalbumin (α-LA) mixtures at pH 5.8, 6.0, 6.5, and 7.0 (A–D, a–d).

were mixed at pH 5.8, the zeta-potential of the mixtures was negative at the LF- $\alpha$ -LA ratios of 1:4, 1:6, and 1:8, and then positive at the ratio of 4:1, 6:1, and 8:1. At the LF- $\alpha$ -LA ratios of 1:2, the charge balance was close to zero. The net-zero charge of LF- $\alpha$ -LA mixtures shifted at higher pH, requiring more LF to balance the higher negative charge of a-LA; at pH 7.0, the optimum mass ratio to achieve neutrality was 4:1 (LF: $\alpha$ -LA). Similar to other studies on the electrostatic complexes (Lin et al., 2022), the optimal mass ratios that were charge neutral were consistent with the ratios that had the highest solution turbidity (Figures 1 and 2S). This indicates that the electrostatic interactions are the primary driving force in LF- $\alpha$ -LA complex formation.

The mean particle sizes of LF- $\alpha$ -LA mixtures were influenced by pH level (Figure 2S). As expected, the LF- $\alpha$ -LA complex size was largest for solutions measured at pH 5.8 and 6.0, specifically at LF to  $\alpha$ -LA ratios of 1:2 at pH 6 and 2:1 at pH 6.5 where the average particle sizes approached 4000 nm, whereas the average size was 260 nm at pH 6.5 at a mass ratio of 1:1 and 100 nm at pH 7.0 at a mass ratio

of 2:1. This data agreed with the visually observed samples and the turbidity and zeta potential data.

The particle size distribution was measured to analyze the particle size uniformity at different complexation conditions (Figure 1S) (Cheong et al., 2016). One prerequisite of complex formation was producing a larger particle size and a unique peak different from either LF or  $\alpha$ -LA. The size distribution by intensity at different pH levels and mass ratios showed large particle size and poor polydispersity index. This phenomenon might be attributed to the scattered distribution of particles, where the large particles, which are over the detection limitation of the instrument, can lead to incorrect results (Xia, 2022).

Based on these results, the optimum conditions for forming LF- $\alpha$ -LA complexes were pH 5.8, 6.0, and 6.5 with LF to a-LA ratios of 1:1, 1:2, and 2:1. Under these conditions, solutions became visibly cloudy, with high turbidity, neutral zeta potential, and large particle sizes. We used these complexes for further studies.



# 3.1.1 | Effect of sodium chloride (NaCl) on the formation of complexes

To probe the nature of the electrostatic interactions between LF and  $\alpha$ -LA in the LF- $\alpha$ -LA complexes, we added salt at various concentrations to the optimized complex solutions (Figure 4S (pH 5.8) and Figure 5S (pH 6.0 and 6.5)). The highest turbidity of LF- $\alpha$ -LA mixtures was at the mass ratios of 1:1 LF to  $\alpha$ -LA at pH 5.8 with 0–50 mM NaCl added. In general, the addition of the salt disfavored the LF- $\alpha$ -LA complex formation, indicating that the interaction of salt ions with proteins may weaken electrostatic interactions between protein molecules (Bastos et al., 2018). For each ratio and pH studied, the interaction of Na<sup>+</sup> and Cl<sup>-</sup> with the proteins masks the reactive sites on the surfaces of the proteins and inhibits the formation of the complex (Souza & Garcia-Rojas, 2017). With further addition of salt, the turbidity decreased and remained at 0.2 after adding 20 mM NaCl in the mixtures at the ratio of 1:1 and 1:2 at pH 5.8. The turbidity of mixtures decreased sharply with the addition of only 10 mM NaCl at pH 6.0 at the LF to  $\alpha$ -LA ratios of 1:1 and 1:2 and at pH 6.5 at the ratio of 2:1. The different salt resistance behavior of LF- $\alpha$ -LA complexes under different pH conditions may result from a change in the proteins hydrophobicity, charge density, or molecular dynamics (Souza & Garcia-Rojas, 2017). In conclusion, a lower salt concentration was likely to promote the electrostatic interactions among polyelectrolytes (Li et al., 2017), and when the salt concentration increased, the turbidity decreased sharply indicative of lower protein-to-protein interactions. Added salts can screen surface charges of proteins, which decreases their electrostatic interaction. Further, salt has been shown to stretch and denature proteins, which causes them to be more soluble (Barbana et al., 2006). Li et al. (2017) reported a similar behavior in the lysozyme complex with carboxymethylcellulose where at low salt concentrations the electrostatic interactions between the two polymers was increased, whereas increased salt concentration decreased the turbidity to nearly zero. Similar phenomena were also observed by Wang et al. (1999) and Seyrek et al. (2003), in which salt reduced the complex coacervation between protein and polyelectrolytes by reducing attractive interactions. The effect of salt concentration on complexation between LF and anionic polysaccharides showed that in mixtures up to 100 mM of salt, an increase in turbidity was observed; beyond 100 mM, the turbidity decreased by Peinado et al. (2010).

# 3.1.2 | Effect of incubation conditions and transglutaminase on the formation of complexes

The yield of all LF- $\alpha$ -LA complexes was lower than 5%, which limits the possible applications for these complexes. To improve the yield of the complexes, the effect of incubation conditions (temperature and time) (Table 1S) and the addition of the cross-linker TG to the optimized samples from the incubation studies (Table 1) on complex yield were studied.

By increasing the incubation temperature from 25 to 45°C, the yield of the LF- $\alpha$ -LA complexes increased slightly within the same period of time (30 min). However, when the incubation time was extended to 4 h, the yield of complex increased by 50% for the three mass ratios observed (Table 1S). An increase in yield of the complex at pH 6.0 with mass ratios 1:1 and 1:2 was achieved after being incubated at 45°C for 4 h, but only a marginal increase in yield was observed by further extending the incubation time to 8 h. Thus, 45°C for 4 h was selected as the optimal incubation temperature and time for complex formation. However, the yields were still poor, the highest vield achieved was 29% after 8 h of incubation at 45°C for the 1:1 complex at pH 6. Therefore, adding a crosslinking agent was then considered to increase complex vield.

TG was used as the cross-linker because it has been shown to effectively enhance the yield of dairy-based products, such as white fresh cheese (García-Gómez et al., 2019) and white-brined cheese (Özer et al., 2013). Ruzengwe et al. (2020) also concluded that TG could enhance the rheological property of groundnut protein hydrogels by forming an organized homogeneous network that promotes the product yield. Consequently, TG was likely to enhance the yield of LF- $\alpha$ -LA complexes and promote thermal stability through the formation of stronger interactions within and between complexes. The higher yield of LF- $\alpha$ -LA complex at pH 6.0, 1:1, and 1:2 was observed by adding 10 mg TG (in 30 mL mixture solution) compared to those without adding TG and adding more TG (30 and 50 mg). But for complexes formed at pH 6.5 with a ratio of 2:1, the addition of TG decreased the yield. The decreased yield of the complex after adding TG was previously reported (García-Gómez et al., 2019), where TG preincubation with protein inhibited the protein interactions during complexation, thus inhibiting further complex formation and micelle aggregation. However, an increased yield in TG-treated complexes was not only achieved by a higher protein retention related to the alteration of the physical properties of the protein

TABLE 1 The yield of lactoferrin (LF)- $\alpha$ -lactalbumin ( $\alpha$ -LA) complex by the addition of transglutaminase (TG) (0, 10, 30 and 50 mg) in 30 mL LF- $\alpha$ -LA mixtures (1 w/v %) followed by incubation at 45°C and 4 h.

	TG added (mg)			
Complex ratios (LF:α-LA)	0 mg (%)	10 mg (%)	30 mg (%)	50 mg (%)
pH 6.5, 2:1	$10.0 \pm 0.7^{a}$	$3.5 \pm 0.3^{b}$	$2.3 \pm 0.3^{b}$	$2.2 \pm 0.2^{b}$
pH 6.0, 1:1	$16.6 \pm 1.7^{a}$	$19.9 \pm 1.1^{a}$	$2.1 \pm 0.3^{b}$	$2.6 \pm 0.2^{b}$
pH 6.0, 1:2	$19.0 \pm 0.4^{b}$	$24.2 \pm 3.9^{a}$	$4.3 \pm 1.7^{d}$	$8.4 \pm 1.6^{\circ}$

*Note*: Different letters indicate the significant levels within each row (p < 0.05).

with a lower pore size but also by increasing the protein fraction (Özer et al., 2013).

Therefore, the optimal conditions for the formation of TG-LF- $\alpha$ -LA complexes at pH 6.0 were 1:1 and 1:2; at pH 6.5, it was 2:1 ratio of LF to LA and incubation at 45°C for 4 h. The addition of TG prior to incubation raised the yield slightly.

### 3.2 | Structure of complex

### 3.2.1 | Fourier-transform infrared spectroscopy (FTIR)

The FTIR was used to investigate the functional groups present in LF- $\alpha$ -LA and the TG-LF- $\alpha$ -LA samples. For native LF, the bands at 1637, 1528, and 1273 cm<sup>-1</sup> represented the amide groups (Barth & Zscherp, 2002), whereas bands for the  $\alpha$ -helix,  $\beta$ -sheets, and random structures for  $\alpha$ -LA appear at 1650/1657 cm<sup>-1</sup> and 1636/1674 cm<sup>-1</sup> (Tarhan et al., 2014).

Based on the current research, amide I is to characterize the secondary structure and C = O stretching vibration of the peptide bonds (Ono et al., 2020). The amide I (1637 cm<sup>-1</sup>) (IV) and amide II (1528 cm<sup>-1</sup>) (III) bonds are in the same position for LF and the LF- $\alpha$ -LA and TG-LF- $\alpha$ -LA complexes indicating that the complexation and cross-linking process had limited influence on the protein structure (Figure 6S A).

By comparing the FTIR spectra of LF and  $\alpha$ -LA complexes with and without TG cross-linking, the strong asymmetric and symmetric stretching vibration of amide bonds at 1528 and 1637 cm $^{-1}$  was apparent, providing preliminary evidence that the complexation process maintained the secondary structure of LF (Figure 6S B). Furthermore, the same vibration bands at 1068 cm $^{-1}$  (I) and 2928 cm $^{-1}$  (VI) in LF and LF- $\alpha$ -LA complexes (without TG added) also indicated that the complexation process maintained the C-C and -CH $_2$  bonds from LF. As far as the influence of TG cross-linking, according to the previous research from Xia (2022), TG cross-linking occurred between the carboxamide group of glutamine and the lysine on the proteins. The vibrational bands at 2360 (V) and 2928 cm $^{-1}$  (VI) in TG

cross-linked samples were contributed from - $\mathrm{CH}_2$ , which indicated cross-link formation. In addition, the change of transmittance in the range 3100–3600 cm $^{-1}$  with a most noticeable band at 3286 cm $^{-1}$  (VII) was attributed to the O–H stretching vibration associated with the reduction of the glutamine residues of the proteins. With the increase of TG added, the transmittance shifted, which indicated that the increased amount of TG cross-linked more proteins and formed stronger covalent bonds. At the same time, the bands at 1068 (I) and 1236 (II) cm $^{-1}$  (II) were due to stretching vibrations of C–C and C–O bonds, which also confirmed the covalent bond formation by TG.

# 3.2.2 | Microstructure analysis of formed complex

The morphology of LF- $\alpha$ -LA complexes formed at pH 6, at 45°C for 4 h, with LF- $\alpha$ -LA ratio of 2:1, 1:1, 1:2, 1:4, and 1:6 (Figure 3A) was characterized to understand the complex formation mechanism between LF and  $\alpha$ -LA. The complex samples were left to settle at room temperature for 2 h, LF- $\alpha$ -LA mixtures at the ratio of 2:1, 1:1, and 1:2 showed sediments in the bottom of the mixtures because of the formation of larger LF- $\alpha$ -LA complex, whereas limited complexes and almost no complex were formed at the ratio of 1:4 and 1:6 (Figure 3A).

The optical microscopy of LF- $\alpha$ -LA complexes shows the complex formed at 2:1 was composed of small amorphous aggregates, whereas the complex formed at 1:1 and 1:2 had larger amorphous particles (Figure 3B). At the ratio of 1:4, the amorphous complex was even smaller and limited, and at the ratio of 1:6, there was almost no particle formation observed. The different observed morphologies were similar to complexes formed by  $\beta$ -conglycinin and lysozyme (Zheng et al., 2021). According to the turbidity study, the optimal ratio to form the LF- $\alpha$ -LA complex was at the ratio around 1:1 and 1:2 at pH 6 when the two proteins had the largest electrostatic interactions. Therefore, the small aggregates formed at 2:1 assembled into large precipitates when more  $\alpha$ -LA was included in the system. When the LF: $\alpha$ -LA ratio reached 1:4 and 1:6, however, excessive

SCHEME 1 The proposed mechanism for lactoferrin (LF)- $\alpha$ -lactalbumin ( $\alpha$ -LA) complex formation.

 $\alpha$ -LA in the system increased the overall negative charges and induced more repulsive forces between the aggregates, thus disfavoring complex formation overall.

The prepared complexes were vacuumed-dried overnight for SEM analysis (Figure 3C). We observed that the LF- $\alpha$ -LA complexes formed nanoparticles (30–50 nm) at the mass ratios of 2:1, 1:1, 1:2, and 1:4 (Figure 3C 1–3). At the ratio of 1:1 and 1:2, larger clusters/sheets were formed because of the aggregation of nanoparticles caused by the drying process. The sediments that formed at a ratio of 2:1 to 1:4 or the complexes at 1:6 were collected by centrifugation and then freeze-dried for SEM analysis (Figure 3D,E).

In general, flake-like particles were displayed in all samples (Figure 3E), which is a typical characteristic of freeze-dried samples (Wang et al., 2017). Spherical microparticles were formed in the complex formed at the ratio of 2:1 to 1:4 (Figure 3E 1-4), whereas this kind of microspheres was not found in the complex formed at the ratio of 1:6. Such formation of microspheres has been reported in the complex formed by two homologous globular proteins,  $\alpha$ -LA and lysozyme (Nigen et al., 2010), and these complex aggregates gradually self-assembled into larger microspheres at certain concentrations following an "aggregation-reorganization" mechanism. As both LF and  $\alpha$ -LA are also homologous globular proteins, we postulate that the freeze-drying process first concentrated the sample, then reorganized the structure of the amorphous LF- $\alpha$ -LA complexes and turned them into spherical microparticles following a similar mechanism.

Given the above microstructure analysis, we propose that the LF- $\alpha$ -LA complex formation mechanism follows the following steps. Initially, LF and  $\alpha$ -LA form soluble, small nanosized complexes driven by electrostatic interactions. When the interactions became stronger, nanocomplexes aggregated to form larger insoluble amorphous clusters also through electrostatic interactions. During the freeze-drying process, some amorphous aggregates reorganized and self-assembled into microspheres. The proposed mechanism is illustrated in Scheme 1.

# 3.3 | Evaluation of thermal stability of complexes

## 3.3.1 | Effect of complexation on the thermal stability of lactoferrin

Our goal was to optimize the complex formation process between LF and  $\alpha$ -LA through electrostatic interactions to enhance thermal stability and retain the functionalities of LF, specifically for use in food applications. We used typical food pasteurization temperatures and times for our thermal studies, these are 2 min at either 75 or 90°C. Because  $\alpha$ -LA is thermally stable at all pH levels, changes in the complex due to pH level changes are understood to be changes in LF thermal stability (Lin et al., 2021). Freezedried samples of the LF- $\alpha$ -LA complexes (2:1, 1:1, and 1:2) formed at pH 6 were chosen because they had the highest yields. Samples were redispersed in the PBS buffer (pH 7.0, 10 mM) at 0.2 w/v % and compared to LF solutions also in the PBS buffer. The thermal stability of LF in LF- $\alpha$ -LA complexes was followed by turbidity, particle size, and solution zeta potential (Figures 2 and 8S).

In the PBS buffer, native LF was a clear solution with low turbidity, small particles, and negative overall charge. Theoretically, the zeta-potential of LF at pH 7 should be positive since the pH was lower than the pI of LF. But the negative charge of LF indicated that the ionic environment caused by the 10 mM PBS influences the surface zeta-potential of LF. Comparing LF with the LF- $\alpha$ -LA complexes, an immediate change of zeta potential to be more negative was observed because  $\alpha$ -LA is negatively charged at this pH. We postulate that because these complexes were made at pH 6 the  $\alpha$ -LA surrounds the LF and masked the usually more positively charged LF.

Samples cross-linked with TG showed an even more negative zeta potential. It was reported that when LF was covalently modified, the pI would be altered (Kroll et al., 2003), where the pI of LF decreased from a higher to a lower pH value after modification since the conjugation of biopolymers on the surface of LF would change the protein surface net charge. This change could further

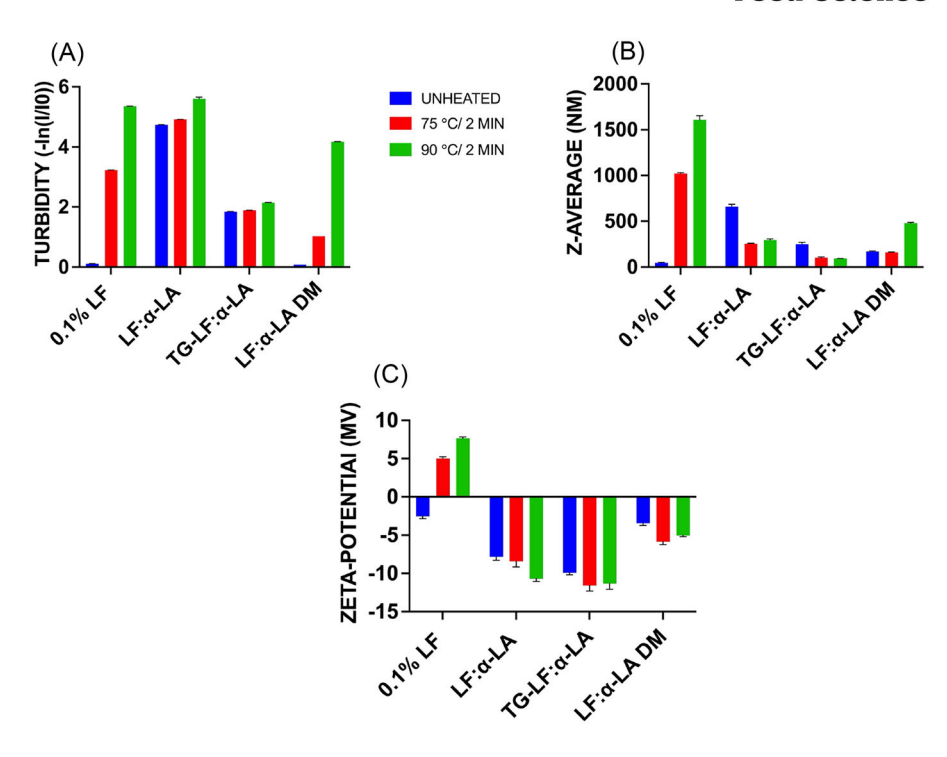


FIGURE 2 Turbidity (a), particle size (b), and zeta-potential (c) change of thermal treated and untreated pH 6.0, lactoferrin (LF)- $\alpha$ -lactalbumin ( $\alpha$ -LA) 1:1 mixtures.

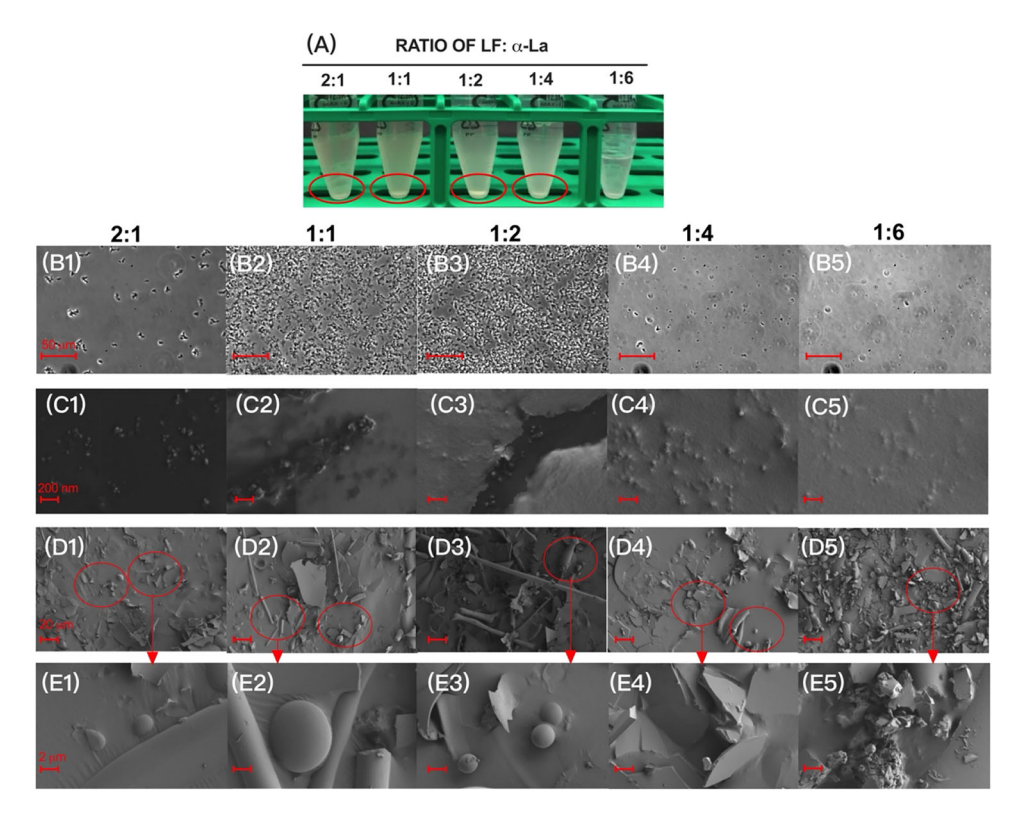


FIGURE 3 Photographic images (a) and optical microscopy images (b) of lactoferrin (LF)– $\alpha$ -lactalbumin ( $\alpha$ -LA) mixtures prepared at pH 6 at different ratios. The scanning electron microscopy (SEM) images of samples after vacuum-drying (c) and after centrifugation and freeze-drying (d and e) regions under the red circles in D are enlarged in E.

influence the surface properties and the availability of the hydrophobic/hydrophobic groups (Liu et al., 2016).

After thermal treatment, the turbidity, mean particle size, and zeta-potential of all LF control samples changed significantly (p < 0.05) (Figure 8S), which was caused by protein thermal aggregation. For native LF, thermal denaturation exposes more hydrophobic sites on the protein surface and accelerated its precipitation and increased the overall mean particle size. The change in the zeta potential may also be attributed to the conformational changes, which change the groups exposed to the solution and therefore increase the positive surface charge (Liu et al., 2020).

For the LF– $\alpha$ -LA complexes, the initial turbidity of the solutions was high but there was little change in particle size and zeta-potential when compared to native LF (Figure 1A). After thermal treatments, however, there was a significant difference in mean particles size (p < 0.05), which was attributed to a decrease in the electrostatic interactions between LF and  $\alpha$ -LA and the expulsion of individual proteins from the complexes (Xu et al., 2019).

After thermal treatment, the TG-LF- $\alpha$ -LA complexes samples showed limited change in turbidity, particle size, and zeta-potential. We attribute this to cross-linking by TG, which hindered dissociation and minimized structural denaturation (Kroll et al., 2003). Direct mixed samples (samples not pH adjusted nor centrifuged) showed increased turbidity and particle size after heating indicating that direct mixing with  $\alpha$ -LA does not protect LF. This further proved that it is the electrostatic-driven complexation between  $\alpha$ -LA and LF that protects LF from thermal denaturation and that TG cross-linking was even more effective at holding the complex together.

In summary, thermal processing reduced the electrostatic interactions between oppositely charged proteins in the complex but the addition of the  $\alpha$ -LA still offered some protection to LF. The effect of the TG cross-linking of the complex further limited the impact of the thermal treatment. The stronger bonding interactions associated with TG cross-linking withstood the thermal treatment and made the TG-LF- $\alpha$ -LA complexes more thermally stable.

# 3.3.2 | Sodium dodecyl sulfate–polyacrylamide gel electrophoresis (SDS–PAGE)

The SDS-polyacrylamide gel electrophoresis (PAGE) of LF and our complexes was used to evaluate the quantity of LF before and after thermal treatment. Based on the research of Lin et al. (2022), LF has a 75 kD molecular weight. The results of SDS-PAGE indicated that all the LF-

 $\alpha$ -LA complexes have the same band around 75 kD (Figure 9S). The presence of this band indicates that the LF- $\alpha$ -LA complexes maintained the polypeptide subunit of LF. The LF- $\alpha$ -LA complexes also exhibited a band at 12.5 kD attributed to  $\alpha$ -LA. The presence of two separate bands in the LF- $\alpha$ -LA complexes, but their different structural and solution properties, is strong evidence of the complex being held together by electrostatic interactions.

For native LF, thermal processing at 75°C for 2 min induced denaturation of the protein, which resulted in a less intense band at 75 kD, whereas after treatment at 90°C for 2 min, the band that represented LF was even less distinct indicating even higher levels of LF denaturation. After the thermal treatments, the unfolding and precipitation of LF formed aggregation, and the upper clear solution was applied for SDS–PAGE. The precipitation of LF comes from the protein denaturation and thermal treatments resulting in the LF unfolded and surface charge decreasing (Darmawan et al., 2020). For the LF and  $\alpha$ -LA direct mixture samples, the phenomenon was similar to the native LF at both temperatures, reinforcing that simply mixing LF with  $\alpha$ -LA does not offer any protection to LF from thermal denaturation.

Thermal treatment of the LF– $\alpha$ -LA complexes at 75°C for 2 min resulted in less significant changes compared with the change observed for native LF, which indicates some protection of LF through complexation with  $\alpha$ -LA was achieved (Figure 10S). However, after treatment at 90°C at 2 min, the denaturation of LF in the LF– $\alpha$ -LA complexes was noticeable, thus only limited protection of LF was observed by the LF– $\alpha$ -LA complexes. For unheated TG cross-linked samples, the aggregation above 250 kD band and another band at 100 kD indicated the formation of larger protein complexes held together by stronger interprotein forces. The cross-linking also provided substantially more stability to these larger complexes after thermal processing both at 75 and 90°C.

# 3.3.3 | Secondary structure change of mixture samples after thermal treatment

#### Intrinsic fluorescence

The intrinsic fluorescence of LF– $\alpha$ -LA complexes before and after thermal treatments was studied to evaluate the conformational changes induced by thermal processing. Protein folding and unfolding can be evaluated by following the fluorescence emission changes of the tryptophan (Trp) residues in LF (Li et al., 2021). When LF precipitates or aggregates, it buries the Trp residue in a hydrophobic cavity, which results in a blue shift of Trp fluorescence. These buried Trp residues are also less available to emit fluorescence and a lower intensity signal is observed (Tan

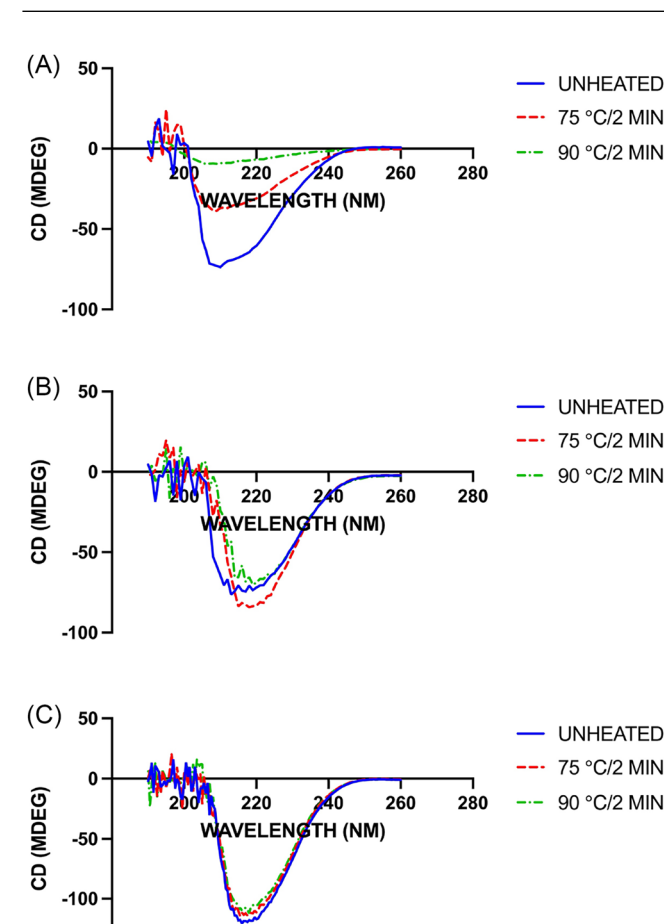


FIGURE 4 Far-UV circular dichroism (CD) spectroscopy. (a) CD spectra of 0.1% (w/v) lactoferrin (LF) in PBS buffer unheated (blue), 75°CC/2 min (red), and 90°C/2 min (green). (b) CD analysis of the 0.2% pH 6.0, 1:1 complex in PBS buffer with unheated, 75°C/2 min and 90°C/2 min treatments. (c) CD analysis of the 0.2% pH 6.0, 1:1 10 mg transglutaminase (TG) in PBS buffer with unheated, 75°C/2 min and 90°C/2 min treatments.

-150 -

et al., 2016). Alternatively, the exposure of Trp during protein unfolding causes a red shift in the Trp intrinsic fluorescence.

Trp residues in the unfolded LF, whether or not LF is complexed or native, have a maximum emission at ~330 nm (Figure 11S). After heating at 90°C, native LF exhibited a redshift of the maximum emission to ~340 nm and an intensity increase. This suggests that the Trp residues of LF were exposed to the aqueous environment during heating (Li et al., 2021). It has been reported that there is no intrinsic fluorescence signal change for  $\alpha$ -LA during thermal treatments, indicating that Trp residues are still buried in the hydrophobic interior of  $\alpha$ -LA (Yang et al., 2021). LF- $\alpha$ -LA complexes formed at pH 6.5 and a ratio of 2:1 showed little change in the maximum of the intrinsic fluorescence but there was a small decrease in intensity after thermal treatment. For 1:1 and 1:2 mass ratios (Figure 12S), the com-

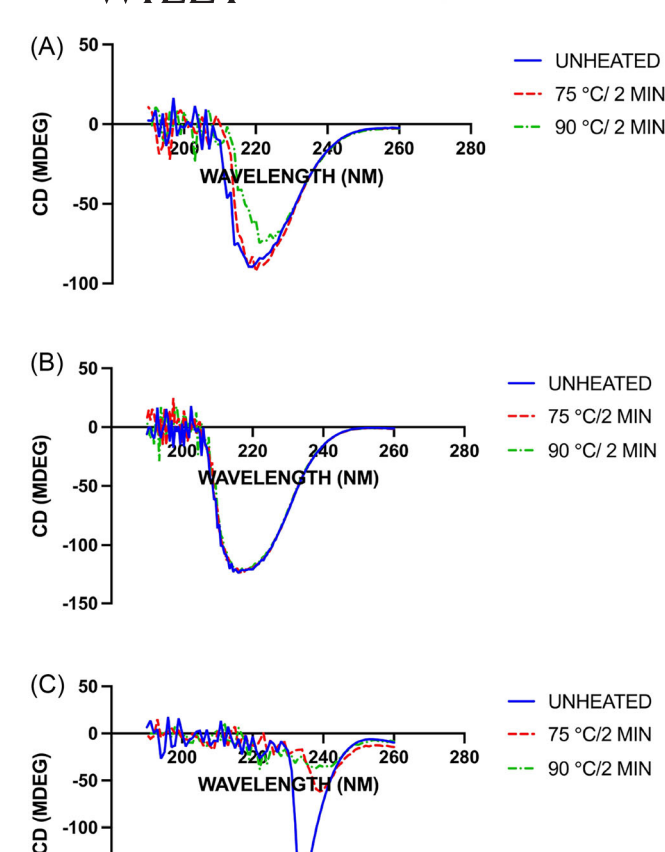
plex showed thermal stability at 75°C for 2 min as there was only limited change of intensity. But after heating at 90°C for 2 min, the intensity of the Trp flouresence increased and redshifted.

The intensity of the intrinsic fluorescence in the TG cross-linked 2:1 complexes decreased after thermal treatments, which is most likely due to the conformation change of the complex that buried the Trp residuals. We attribute this to stronger associations such as stronger hydrophobic interactions or additional thermally induced cross-linking between LF and  $\alpha$ -LA that was facilitated by the initial TG cross-linking. This phenomenon has been reported in the complexation between carbonyl groups of polysaccharides with the amino groups of proteins (Chang et al., 2017, 2018). The mean particle size decreased significantly (p < 0.05) for TG cross-linked LF- $\alpha$ -LA 1:2 complex made at pH 6, from 352 nm to 234 nm after 75 and at 90°C, the mean size further decreased to 214 nm (Figure 2). We postulate that thermal treatment caused the  $\alpha$ -LA to wind around the LF core, which was again facilitated by the proximity of the two proteins due to TG cross-linking.

#### Far-UV circular dichroism (CD)

The secondary structure change of LF after complexation and heating (75 or 90°C for 2 min) was determined by Far-UV CD spectroscopy to uncover the folding and binding properties of the proteins and complexes that may be occurred (Yang et al., 2021). The far-UV CD of LF- $\alpha$ -LA complexes was compared to that of LF (Table 2S). LF contained a relatively high content of  $\beta$ -sheets (27.7%–30.1%) but was low in  $\alpha$ -helix structure (17.6%–18.3%). The direct mixtures of LF and  $\alpha$ -LA all presented a decrease in  $\alpha$ -helix structure or an increase in  $\beta$ -sheet content regardless of mass ratio, which may have resulted from the introduction of  $\alpha$ -LA. Similar to LF- $\alpha$ -LA complexes, increasing α-LA concentrations had no influence on LF secondary structure (Figure 4). A positive band identifies the  $\alpha$ -helical structure of LF at 190 nm and an intense negative band at 208 nm with a 220 nm shoulder (Tu et al., 2020).

Upon heating, the 0.1 w/v% solution of LF showed an increase in  $\beta$ -sheet content, from 27.7% for unheated to 30.3% for 75°C and 36.4% for 90°C, whereas  $\alpha$ -helical content decreased from 17.6% for unheated to 15.2% for 75°C and 8.8% for heated at 90°C. Consequently, the difference in structural characteristics between heated and unheated samples confirmed the protein aggregation and stability after thermal treatments. After heating, the LF- $\alpha$ -LA complexes showed an increase in  $\beta$ -sheet structure. Hydrogen bonds mainly stabilize  $\beta$ -sheet; therefore, the increase in the amount of  $\beta$ -sheets in the complexes indicates that the complexation with  $\alpha$ -LA enhances the hydrogen bonding in the complexes during thermal treatments (Yang et al., 2021). To support this, we noticed an increase of  $\alpha$ -helix



Far-UV circular dichroism (CD) spectroscopy. (a) CD spectra of 0.2% (w/v) lactoferrin (LF)- $\alpha$ -lactalbumin ( $\alpha$ -LA) 1:2 in PBS buffer unheated (blue), 75°C/2 min (red), and 90°C/2 min (green). (b) CD analysis of the 0.2% transglutaminase (TG)-LF- $\alpha$ -LA 1:2 in PBS buffer with unheated, 75°C/2 min and 90°C/2 min treatments. (c) CD analysis of the 0.2% LF- $\alpha$ -LA 1:2 direct mix (DM) samples in PBS buffer with unheated, 75°C/2 min and 90°C/2 min treatments.

-100

-150

-200

structure in complexes with 1:1 and 1:2 (LF to  $\alpha$ -LA mass ratios), whereas complexes with higher amounts of LF (2:1) retained their  $\beta$ -sheet structure through the thermal processing (Figures 5 and 16S).

The TG cross-linked samples showed better retention of the LF secondary structure throughout thermal processing with the least change in CD spectra. After thermal treatment at 75°C, all TG-LF-α-LA samples protected LF (Table 2S). When the TG-LF- $\alpha$ -LA complexes at a 2:1 ratio were heated at 90°C, the cross-linked samples exhibited a slight secondary structure change. When TG-LF- $\alpha$ -LA complexes with a 1:2 ratio were heated, the  $\beta$ -sheet increased from 27.5% to 34.4%, and the random coil decreased from 40.9% to 37.5%. Overall, thermal treatments induced a change in the secondary structure of LF itself. The LF- $\alpha$ -LA complexes and TG cross-linked complexes

presented better protection on the secondary structure of LF after heating as the CD changes were limited and less than those observed for native LF samples. The TG-LF- $\alpha$ -LA cross-linked samples proved to have the best protection for LF regarding the retention of its secondary structures.

### 3.4 | Effect of complexation on the antibacterial activity of LF

To analyze the protection of LF functionality (antibacterial properties) through complexation, before and after thermal treated LF,  $\alpha$ -LA, LF- $\alpha$ -LA, and TG-LF- $\alpha$ -LA complexes were investigated. S. aureus and E. coli are common bacteria in the food industry and were used as the target Gram positive (G+) and Gram negative (G-) bacteria. After incubating for 24 h, both LF, LF- $\alpha$ -LA complexes, and TG-LF- $\alpha$ -LA cross-linked complexes significantly (p < 0.05) reduced the growth of G+ and G- bacteria compared with the control group (PBS only), whereas the  $\alpha$ -LA group had no significant (p < 0.05) difference with respect to the control group (Figures 6 and 17S). After thermal treatment for 2 min at 75°C, LF was significantly less effective in reducing bacterial growth (p < 0.05) (Figures 6 and 17S). Unheated LF- $\alpha$ -LA complexes showed antibacterial activity toward G + and G- bacteria (Figures 18S and 19S), and after thermal treatment, the antibacterial activity of LF in LF- $\alpha$ -LA complexes was retained. The highest resistance to temperature processing was found for the TG-LF- $\alpha$ -LA samples, which exhibited the best antibacterial activity after thermal treatment (Figures18S and 19S). This is likely due to the structural reinforcement attributed by TG to the LF- $\alpha$ -LA complexes, the denser structure maintained the LF structure and protected the antibacterial activity of LF through thermal treatments (Salinas-Valdés et al., 2015).

Our results demonstrate that the complexation of LF with  $\alpha$ -LA maintains LF's antibacterial activity and that the complexes provide some protection toward LF during thermal processing. Cross-linking of the complexes with TG reinforced the complex structure and helped to retain LF's antibacterial activity after thermal processing.

#### 4 CONCLUSION

We have demonstrated that  $\alpha$ -LA could be used to form complexes with LF that enhance thermal stability as well as retain the functionality of LF. Complexes were formed at pH levels between 5.8 and 7.0 with varying mass ratios. The optimal complexation condition was achieved at pH 6.0 and a mass ratio of 1:2 (LF to  $\alpha$ -LA) with 10 mg of TG added. The addition of TG was used to increase the

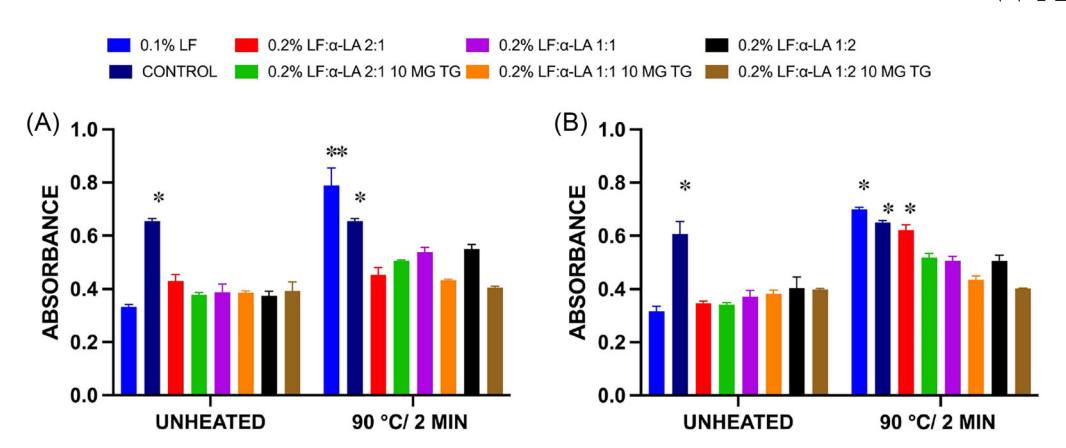


**FIGURE 6** The effect of complexation and thermal treatment (90°C/2 min) on antibacterial capacity (*Staphylococcus aureus* (*S. aureus*) (a), *Escherichia coli* (*E. coli*) (b)) of lactoferrin (LF)– $\alpha$ -lactalbumin ( $\alpha$ -LA) complexes after incubation for 24 h. (\* and \*\* indicate the different significant levels, \* p < 0.01, \*\* p < 0.001).

complex yield and to provide additional thermal stability to the complexes. We were able to confirm that LF and a-LA form an electrostatic complex when centrifuged at pH 6 in a 1:2 LF to a-LA ratio. The addition of TG crosslinked the two proteins and added additional stability. The SDS-PAGE confirmed the electrostatic interactions between LF and a-LF and the stronger, potentially covalent interactions between TG, LF, and a-LA in the TG-LF- $\alpha$ -LA cross-linked complexes. The cross-linked complexes were more resistant to thermal processing, and the antibacterial properties of LF were retained even after thermal treatment. The promising outcomes of this study would provide the industry with available commercialization methods to utilize LF and expand the application conditions for consumers.

#### **AUTHOR CONTRIBUTIONS**

Yufeng Zhou and Tiantian Lin: Conceptualization; data curation; formal analysis; investigation; methodology; writing—review and editing; writing—original draft. Younas Dadmohammadi: Project administration; conceptualization; writing—review and editing. Peilong Li; Hongmin Dong; Yanhong He; and Lixin Yang: Investigation. Gopinathan Meletharayil and Rohit Kapoor: Resources; writing—review and editing. Alireza Abbaspourrad: Supervision; resources; funding acquisition; writing—review and editing.

#### **ACKNOWLEDGMENTS**

The authors would like to acknowledge Dairy Management, Inc. (Rosemont, IL, USA) for the funding support. The authors would like to thank the assistance and technical support from Dr. Crane and Rebecca Zawistowski in CD spectroscopy. Materials from this research on SEM were provided from Cornell Center for Materials Research

(CCMR), which is supported by National Science Foundation under Award Number DMR-1719875.

#### CONFLICT OF INTEREST STATEMENT

The authors declare no conflicts of interest.

#### ORCID

Tiantian Lin https://orcid.org/0000-0002-1816-3380 Alireza Abbaspourrad https://orcid.org/0000-0001-5617-9220

#### REFERENCES

Barbana, C., Pérez, M. D., Sánchez, L., Dalgalarrondo, M., Chobert, J. M., Haertlé, T., & Calvo, M. (2006). Interaction of bovine -lactalbumin with fatty acids as determined by partition equilibrium and fluorescence spectroscopy. *International Dairy Journal*, *16*(1), 18–25. https://doi.org/10.1016/j.idairyj.2005.01.007

Barth, A., & Zscherp, C. (2002). What vibrations tell about proteins. *Quarterly Reviews of Biophysics*, *35*(4), 369–430. https://doi.org/10.1017/S0033583502003815

Bastos, L. P. H., de Carvalho, C. W. P., & Garcia-Rojas, E. E. (2018). Formation and characterization of the complex coacervates obtained between lactoferrin and sodium alginate. *International Journal of Biological Macromolecules*, 120, 332–338. https://doi. org/10.1016/j.ijbiomac.2018.08.050

Bengoechea, C., Jones, O. G., Guerrero, A., & McClements, D. J. (2011). Formation and characterization of lactoferrin/pectin electrostatic complexes: Impact of composition, pH and thermal treatment. *Food Hydrocolloids*, *25*(5), 1227–1232. https://doi.org/10.1016/j.foodhyd.2010.11.010

Chang, C., Wang, T., Hu, Q., & Luo, Y. (2017). Caseinate-zein-polysaccharide complex nanoparticles as potential oral delivery vehicles for curcumin: Effect of polysaccharide type and chemical cross-linking. *Food Hydrocolloids*, 72, 254–262. https://doi.org/10.1016/j.foodhyd.2017.05.039

Chen, H., Ji, A., Qiu, S., Liu, Y., Zhu, Q., & Yin, L. (2018).
Covalent conjugation of bovine serum album and sugar beet pectin through Maillard reaction/laccase catalysis to improve the

- emulsifying properties. Food Hydrocolloids, 76, 173–183. https://doi.org/10.1016/j.foodhyd.2016.12.004
- Cheong, A. M., Tan, K. W., Tan, C. P., & Nyam, K. L. (2016). Kenaf (*Hibiscus cannabinus* L.) seed oil-in-water Pickering nanoemulsions stabilised by mixture of sodium caseinate, Tween 20 and β-cyclodextrin. *Food Hydrocolloids*, *52*, 934–941. https://doi.org/10. 1016/j.foodhyd.2015.09.005
- Darmawan, K. K., Karagiannis, T. C., Hughes, J. G., Small, D. M., & Hung, A. (2020). High temperature induced structural changes of apo-lactoferrin and interactions with  $\beta$ -lactoglobulin and  $\alpha$ -lactalbumin for potential encapsulation strategies. *Food Hydrocolloids*, *105*, 105817. https://doi.org/10.1016/j.foodhyd.2020. 105817
- García-Gómez, B., Vázquez-Odériz, M. L., Muñoz-Ferreiro, N., Romero-Rodríguez, M. Á., & Vázquez, M. (2019). Interaction between rennet source and transglutaminase in white fresh cheese production: Effect on physicochemical and textural properties. LWT, 113, 108279. https://doi.org/10.1016/j.lwt.2019. 108279
- Harouna, S., Franco, I., Carramiñana, J. J., Blázquez, A., Abad, I., Pérez, M. D., Calvo, M., & Sánchez, L. (2020). Effect of hydrolysis and microwave treatment on the antibacterial activity of native bovine milk lactoferrin against *Cronobacter sakazakii*. *International Journal of Food Microbiology*, 319, 108495. https://doi.org/ 10.1016/j.ijfoodmicro.2019.108495
- Huppertz, T., Fox, P. F., & Kelly, A. L. (2004). High pressure-induced denaturation of  $\alpha$ -lactalbumin and  $\beta$ -lactoglobulin in bovine milk and whey: A possible mechanism. *Journal of Dairy Research*, 71(4), 489–495. https://doi.org/10.1017/S0022029904000500
- Jenssen, H., & Hancock, R. (2009). Antimicrobial properties of lactoferrin. *Biochimie*, 91(1), 19–29. https://doi.org/10.1016/j.biochi. 2008.05.015
- Kehoe, J. J., & Brodkorb, A. (2014). Interactions between sodium oleate and  $\alpha$ -lactalbumin: The effect of temperature and concentration on complex formation. *Food Hydrocolloids*, 34, 217–226. https://doi.org/10.1016/j.foodhyd.2012.09.009
- Kroll, J., Rawel, H. M., & Rohn, S. (2003). Reactions of plant phenolics with food proteins and enzymes under special consideration of covalent bonds. Food Science and Technology Research, 9(3), 205–218. https://doi.org/10.3136/fstr.9.205
- Li, Y., Zhang, Z., & Abbaspourrad, A. (2021). Improved thermal stability of phycocyanin under acidic conditions by forming soluble complexes with polysaccharides. *Food Hydrocolloids*, *119*, 106852. https://doi.org/10.1016/j.foodhyd.2021.106852
- Li, Z., Wang, Y., Pei, Y., Xiong, W., Xu, W., Li, B., & Li, J. (2017). Effect of substitution degree on carboxymethylcellulose interaction with lysozyme. *Food Hydrocolloids*, 62, 222–229. https://doi.org/10.1016/j.foodhyd.2016.07.020
- Lin, T., Dadmohammadi, Y., Davachi, S. M., Torabi, H., Li, P., Pomon, B., Meletharayil, G., Kapoor, R., & Abbaspourrad, A. (2022). Improvement of lactoferrin thermal stability by complex coacervation using soy soluble polysaccharides. *Food Hydrocolloids*, *131*, 107736. https://doi.org/10.1016/j.foodhyd.2022.107736
- Lin, T., Meletharayil, G., Kapoor, R., & Abbaspourrad, A. (2021). Bioactives in bovine milk: Chemistry, technology, and applications. *Nutrition Reviews*, 79(Suppl\_2), 48–69. https://doi.org/10.1093/nutrit/nuab099
- Liu, F., Wang, D., Ma, C., & Gao, Y. (2016). Conjugation of polyphenols prevents lactoferrin from thermal aggregation at neutral pH.

- Food Hydrocolloids, 58, 49–59. https://doi.org/10.1016/j.foodhyd. 2016.02.011
- Liu, J., Yang, J., Abliz, A., Mao, L., Yuan, F., & Gao, Y. (2020). Influence of thermal treatment on physical, structural characteristics and stability of lactoferrin, EGCG and high methoxylated pectin aggregates. *LWT*, 125, 109221. https://doi.org/10.1016/j.lwt. 2020.109221
- Matsumura, Y., Lee, D.-S., & Mori, T. (2000). Molecular weight distributions of a-lactalbumin polymers formed by mammalian and microbial transglutaminases. *Food Hydrocolloids*, 14, 49–59. https://doi.org/10.1016/S0268-005X(99)00045-4
- McCarthy, N. A., Kelly, A. L., O'Mahony, J. A., & Fenelon, M. A. (2014). Sensitivity of emulsions stabilised by bovine β-casein and lactoferrin to heat and CaCl2. *Food Hydrocolloids*, *35*, 420–428. https://doi.org/10.1016/j.foodhyd.2013.06.021
- Nedovic, V., Kalusevic, A., Manojlovic, V., Levic, S., & Bugarski, B. (2011). An overview of encapsulation technologies for food applications. *Procedia Food Science*, *1*, 1806–1815. https://doi.org/10.1016/j.profoo.2011.09.265
- Nicolai, T. (2016). Formation and functionality of self-assembled whey protein microgels. *Colloids and Surfaces B: Biointerfaces*, *137*, 32–38. https://doi.org/10.1016/j.colsurfb.2015.05.055
- Nigen, M., Gaillard, C., Croguennec, T., Madec, M.-N., & Bouhallab, S. (2010). Dynamic and supramolecular organisation of αlactalbumin/lysozyme microspheres: A microscopic study. *Biophysical Chemistry*, 146(1), 30–35. https://doi.org/10.1016/j.bpc. 2009.10.001
- Ono, K., Sakai, H., Tokunaga, S., Sharmin, T., Aida, T. M., & Mishima, K. (2020). Encapsulation of lactoferrin for sustained release using particles from gas-saturated solutions. *Processes*, 9(1), 73. https:// doi.org/10.3390/pr9010073
- Özer, B., Hayaloglu, A. A., Yaman, H., Gürsoy, A., & Şener, L. (2013). Simultaneous use of transglutaminase and rennet in white-brined cheese production. *International Dairy Journal*, *33*(2), 129–134. https://doi.org/10.1016/j.idairyj.2013.02.001
- Peinado, I., Lesmes, U., Andrés, A., & McClements, J. D. (2010). Fabrication and morphological characterization of biopolymer particles formed by electrostatic complexation of heat treated lactoferrin and anionic polysaccharides. *Langmuir*, 26(12), 9827–9834. https://doi.org/10.1021/la1001013
- Ruzengwe, F. M., Amonsou, E. O., & Kudanga, T. (2020). Transglutaminase-mediated crosslinking of Bambara groundnut protein hydrogels: Implications on rheological, textural and microstructural properties. *Food Research International*, 137, 109734. https://doi.org/10.1016/j.foodres.2020.109734
- Salinas-Valdés, A., De la Rosa Millán, J., Serna-Saldívar, S. O., & Chuck-Hernández, C. (2015). Yield and textural characteristics of panela cheeses produced with dairy-vegetable protein (soybean or peanut) blends supplemented with transglutaminase: Panela cheese with vegetable proteins. *Journal of Food Science*, 80(12), S2950–S2956. https://doi.org/10.1111/1750-3841.13126
- Seyrek, E., Dubin, P. L., Tribet, C., & Gamble, E. A. (2003). Ionic strength dependence of protein-polyelectrolyte interactions. *Biomacromolecules*, 4(2), 273–282. https://doi.org/10.1021/bm025664a
- Souza, C. J. F., & Garcia-Rojas, E. E. (2017). Interpolymeric complexing between egg white proteins and xanthan gum: Effect of salt and protein/polysaccharide ratio. *Food Hydrocolloids*, 66, 268–275. https://doi.org/10.1016/j.foodhyd.2016.11.032

- Taheri-Kafrani, A., Gaudin, J.-C., Rabesona, H., Nioi, C., Agarwal, D., Drouet, M., Chobert, J.-M., Bordbar, A.-K., & Haertle, T. (2009). Effects of heating and glycation of  $\beta$ -lactoglobulin on its recognition by IgE of sera from cow milk allergy patients. Journal of Agricultural and Food Chemistry, 57(11), 4974-4982. https://doi. org/10.1021/jf804038t
- Tan, C., Feng, B., Zhang, X., Xia, W., & Xia, S. (2016). Biopolymercoated liposomes by electrostatic adsorption of chitosan (chitosomes) as novel delivery systems for carotenoids. Food Hydrocolloids, 52, 774-784. https://doi.org/10.1016/j.foodhyd.2015.08.016
- Tarhan, Ö., Tarhan, E., & Harsa, S. (2014). Investigation of the structure of alpha-lactalbumin protein nanotubes using optical spectroscopy. Journal of Dairy Research, 81(1), 98-106. https://doi. org/10.1017/S0022029913000629
- Tu, Y., Xu, Y., Ren, F., & Zhang, H. (2020). Characteristics and antioxidant activity of Maillard reaction products from  $\alpha$ -lactal burnin and 2'-fucosyllactose. Food Chemistry, 316, 126341. https://doi.org/10. 1016/j.foodchem.2020.126341
- Wang, B., Timilsena, Y. P., Blanch, E., & Adhikari, B. (2017). Characteristics of bovine lactoferrin powders produced through spray and freeze drying processes. International Journal of Biological Macromolecules, 95, 985-994. https://doi.org/10.1016/j.ijbiomac.2016.10.
- Wang, Y., Kimura, K., Huang, Q., Dubin, P. L., & Jaeger, W. (1999). Effects of salt on polyelectrolyte-micelle coacervation. Macromolecules, 32(21), 7128-7134. https://doi.org/10.1021/ma990972v
- Xia, T. (2022). Lactoferrin particles assembled via transglutaminaseinduced crosslinking: Utilization in oleogel-based Pickering emulsions with improved curcumin bioaccessibility. Food Chemistry. 374, 131779. https://doi.org/10.1016/j.foodchem.2021.131779
- Xu, K., Zhao, Z., Guo, M., & Du, J. (2019). Conjugation between okra polysaccharide and lactoferrin and its inhibition effect on thermal aggregation of lactoferrin at neutral pH. LWT, 107, 125–131. https:// doi.org/10.1016/j.lwt.2019.02.082

- Yang, W., Qu, X., Deng, C., Dai, L., Zhou, H., Xu, G., Li, B., Yulia, N., & Liu, C. (2021). Heat sensitive protein-heat stable protein interaction: Synergistic enhancement in the thermal co-aggregation and gelation of lactoferrin and α-lactalbumin. Food Research International, 142, 110179. https://doi.org/10.1016/j.foodres.2021. 110179
- Yang, W., Xu, C., Liu, F., Yuan, F., & Gao, Y. (2014). Native and thermally modified protein-polyphenol coassemblies: Lactoferrinbased nanoparticles and submicrometer particles as protective vehicles for (-)-epigallocatechin-3-gallate. Journal of Agricultural and Food Chemistry, 62(44), 10816-10827, https://doi.org/10.1021/ jf5038147
- Zheng, J., Gao, Q., Ge, G., Wu, J., Tang, C., Zhao, M., & Sun, W. (2021). Heteroprotein complex coacervate based on  $\beta$ conglycinin and lysozyme: Dynamic protein exchange, thermodynamic mechanism, and lysozyme activity. Journal of Agricultural and Food Chemistry, 69(28), 7948-7959. https://doi.org/10.1021/ acs.jafc.1c02204

#### SUPPORTING INFORMATION

Additional supporting information can be found online in the Supporting Information section at the end of this article.

How to cite this article: Zhou, Y., Lin, T., Dadmohammadi, Y., Li, P., Dong, H., Yang, L., He, Y., Meletharayil, G., Kapoor, R., & Abbaspourrad, A. (2024). Using transglutaminase to cross-link complexes of lactoferrin and  $\alpha$ -lactalbumin to increase thermal stability. Journal of Food Science, 1-15. https://doi.org/10.1111/1750-3841.17182